polymers

MDPI

Article

Bioreducible Micelles Self-Assembled from Poly(ethylene glycol)-Cholesteryl Conjugate As a Drug Delivery Platform

Chulsu Baek †, Tae-Lin Ha †, Eunjoo Kim, Sang Won Jeong, Se Guen Lee, Sung Jun Lee and Hyun-Chul Kim *

Received: 22 September 2015 ; Accepted: 30 October 2015 ; Published: 6 November 2015
Academic Editor: Michael K.C. Tam

Division of Nano and Energy Convergence Research, Daegu Gyeongbuk Institute of Science and Technology (DGIST), Daegu 711-873, Korea; baek384@dgist.ac.kr (C.B.); taelin@dgist.ac.kr (T.-L.H.); ejkim@dgist.ac.kr (E.K.); sjeong@dgist.ac.kr (S.W.J.); sklee@dgist.ac.kr (S.G.L.); schrisj@dgist.ac.kr (S.J.L.)
* Correspondence: kimhc@dgist.ac.kr; Tel.: +82-53-785-2540; Fax: +82-53-785-3559
† These authors contributed equally to this work.

Abstract: The ability of polymeric micelles to self-assemble into nanosized particles has created interest in their application as potential anticancer drug delivery systems. A poly(ethylene glycol)-cholesteryl conjugate (Chol-ss-PEG-ss-Chol) connected by cleavable disulfide linkages was synthesized and used as a nanocarrier for *in vitro* release of doxorubicin (DOX). Owing to its amphiphilic structure, Chol-ss-PEG-ss-Chol was able to self-assemble into micelles with an average diameter 18.6 nm in aqueous solution. The micelles formed large aggregates due to the shedding of the PEG shell through cleavage of disulfide bonds in a reductive environment. The *in vitro* release studies revealed that Chol-ss-PEG-ss-Chol micelles released 80% and approximately 9% of the encapsulated DOX within 6 h under reductive and non-reductive conditions, respectively. The glutathione (GSH)-mediated intracellular drug delivery was investigated in a KB cell line. The cytotoxicity of DOX-loaded micelles indicated a higher cellular anti-proliferative effect against GSH-pretreated than untreated KB cells. Furthermore, confocal laser scanning microscopy (CLSM) measurement demonstrated that Chol-ss-PEG-ss-Chol micelles exhibited faster drug release in GSH-pretreated KB cells than untreated KB cells. These results suggest the potential usefulness of disulfide-based polymeric micelles as controlled drug delivery carriers.

Keywords: polymeric micelles; drug delivery system; biocompatible; disulfide-thiol exchange; stimulus-sensitive polymers

1. Introduction

Polymeric micelles have attracted significant attention as anticancer drug carriers because they can self-assemble into nanosized micelles in water [1–3]. These micelles provide enhanced stability for lengthy drug circulation in blood owing to their low critical micelle concentration (CMC), followed by drug accumulation in solid tumors through an enhanced permeability and retention effect (EPR) [2,4–6]. Among the various types of micelles, amphiphilic copolymers comprised of poly(ethylene glycol) (PEG) as the hydrophilic segments and polyesters including poly(D,L-lactic acid) (PDLLA), poly(glycolic acid) (PGA), and poly(ε-caprolactone) (PCL) as the hydrophobic segments have been extensively investigated as drug carriers due to their excellent biocompatibility and biodegradability [7–13]. However, the drug release inside cancer cells is often insufficient due to the highly hydrophobic and slow degrading nature of inner core-forming polyesters, which results in slow and incomplete drug release [14,15]. In addition, it has been reported that PEG

brushes or clouds, which act as steric barriers to drug release and cell uptake, can be formed when PEG is used as the micelle hydrophilic shell [16–18]. These drawbacks may be improved by using amphiphilic copolymers with elements that cleave in response to external stimuli such as pH, redox, and temperature. Among the various cleavable linkages, disulfide-thiol exchange reaction is a remarkable stimuli-responsive platform because disulfide linkages are cleaved to the corresponding thiols by reducing agents such as glutathione (GSH), cysteine, and DL-dithiothreitol (DTT) [19]. In biological systems, GSH, a cysteine-containing tripeptide capable of reducing disulfide linkages, is found in extracellular (~2 μM) and intracellular (1–10 mM) compartments at concentrations, known to be several times higher in tumors than they are in healthy tissues [20]. Therefore, amphiphilic copolymers containing disulfide linkages within the hydrophobic backbone or a single disulfide bond at the connection of the two polymer blocks have been prepared for use in redox-responsive drug delivery [21–24]. However, the preparation of disulfide-bearing polymers is often complex because it requires thiol-disulfide exchange reactions to introduce disulfide bonds at the junctions or the side chains of diblock copolymers. This is attributable to the instability of free thiols that makes them capable of oxidizing under ambient conditions.

In this study, we evaluated poly(ethylene glycol)-cholesteryl conjugate (Chol-ss-PEG-ss-Chol)-based shell-sheddable micelles containing a disulfide bond at the junction of the hydrophilic corona and hydrophobic core. This amphiphile was prepared using facile synthetic procedures. PEG-cholesteryl conjugates are often used as drug carrier owing to their excellent biocompatibility with host molecules, low toxicity, and high solution stability at their CMC [18]. Although pH-sensitive PEG-cholesteryl conjugates have been studied to determine if they exhibit complete drug release inside cancer cells [25,26], there are no previous reports of PEG-cholesteryl conjugates with cleavable linkage in response to thiols. Therefore, we investigated the disintegration or destabilization of Chol-ss-PEG-ss-Chol micelles following cleavage of disulfide in the presence of DTT using NMR, gel permeation chromatography (GPC), and dynamic light scattering (DLS). Their destabilization enhanced the release of encapsulated doxorubicin (DOX), a hydrophobic anticancer drug. Furthermore, their GSH-responsive destabilization was investigated in KB cell lines using confocal laser scanning microscopy (CLSM) to monitor cellular uptake as well as cell viability assays to evaluate anticancer efficacy.

2. Experimental Section

2.1. Materials

Poly(ethylene glycol) (PEG) with a molecular weight of 3400 g/mol, cystamine dihydrochloride (96%), di-*tert*-butyldicarbonate (99%), succinic anhydride (99%), trifluoroacetic acid (TFA, 99%), *N*,*N*′-dicyclohexylcarboiimide (DCC, 99%), triethylamine (TEA, 99.9%), and cholesteryl chloroformate (95%), DL-dithiothreitol (DTT, 99%) were purchased from Sigma–Aldrich (St. Louis, MO, USA) and used as received. All solvents were obtained from commercial suppliers and were used without further purification. KB cells were purchased from the American Type Culture Collection (ATCC, Manassas, VA, USA). Eagle's minimum essential medium (EMEM) was obtained from Life Technologies (Carlsbad, CA, USA). Trypsin-ethylenediaminetetraacetic acid (EDTA, 0.25%) and fetal bovine serum (FBS) were purchased from HyClone Laboratories (Logan, UT, USA). A Cell Counting Kit-8 (CCK-8) was obtained from Enzo Life Science (New York, NY, USA). Glutathione-reduced ethyl ester (GSH-OEt) was purchased from Sigma–Aldrich (St. Louis, MO, USA).

2.2. Measurements

Nuclear magnetic resonance (NMR) spectra were obtained using a Bruker NMR spectrometer (AVANCE III 400, Billerica, MA, USA). The molecular weight and molecular weight distribution of the polymer were determined using gel permeation chromatography (GPC, Waters, Milford, MA,

USA) equipped with a Waters 2414 refractive index detector and Waters Styragel HR columns. Tetrahydrofuran (THF) was used as the mobile phase (flow rate: 1 mL/min, at 35 °C) and column calibration was performed with polystyrene standards. The size and size distribution based on the intensity were measured using dynamic light scattering (DLS, Zetasizer Nano ZS, Malvern Instruments, Malvern, Worcestershire, UK). The nanostructure of the nanoparticles was examined using transmission electron microscopy (TEM, HF-3300, Hitachi, Chiyoda-ku, Tokyo, Japan). The samples were negatively stained on a 300 mesh copper grid with 2 wt % phosphotungstic acid hydrate and ultraviolet-visible (UV-VIS) absorption spectra were obtained using a Cary 100 Conc UV-VIS spectrometer (Varian, Palo Alto, CA, USA).

2.3. Synthesis

Mono-Boc-cystamine: This was prepared as previously described [27]. Briefly, cystamine dihydrochloride (8.0 g, 36 mmol) was dissolved in methanol (200 mL) and TEA (15.0 mL, 107.7 mmol) was added, followed by di-*tert*-butyldicarbonate (7.7 g, 36 mmol). The mixture was stirred for 1 h at room temperature and then the solvent was evaporated *in vacuo*. To the residue, 1 M monosodium phosphate (NaH_2PO_4, 80 mL, pH = 4.2) was added, and the mixture was extracted twice with diethyl ether to remove di-Boc-cystamine. The aqueous solution was basified (pH = 9) with 1 M sodium hydroxide (NaOH) and extracted twice with ethyl acetate. The combined organic phases were washed twice with water, dried, and evaporated *in vacuo* to yield 3.3 g (13.4 mmol, 37.3%) of mono-Boc-cystamine. The proton (^{1}H NMR δ (ppm)) spectral characteristics were: 5.03 (s, 1H, –NH), 3.44 (d, 2H, NHCH_2), 3.01 (t, 2H, –CH_2NH_2), 2.78 (d, 4H, –CH_2SSCH_2-), 1.44 (s, 9H, –O(CH_3)$_3$).

α,ω-Carboxylic-modified PEG (HOOC-PEG-COOH): PEG (3.4 g, 1 mmol) and succinic anhydride (0.3 g, 3.0 mmol) were dissolved in chloroform ($CHCl_3$, 50 mL), and TEA (0.3 mL, 2.2 mmol) was added to the solution. The mixture was refluxed at 70 °C for 24 h and then was washed twice with water. The resulting product was precipitated in an excess amount of cold diethyl ether. The precipitate was filtered, washed several times with diethyl ether, and then vacuum-dried to obtain HOOC-PEG-COOH with a yield of 3.3 g and the following ^{1}H NMR δ (ppm) spectral characteristics: 4.24 (t, 2H, –OCH_2CH_2O(CO)–), 3.66 (PEG), 2.63 (m, 4H, –(CO)CH_2CH_2COOH).

α,ω-(Mono-Boc-cystamine)-modified PEG (Boc-ss-PEG-ss-Boc): HOOC-PEG-COOH (2.0 g, 0.56 mmol) and mono-Boc-cystamine (0.3 g, 1.20 mmol) was dissolved in anhydrous dichloromethane (30 mL), and DCC (0.25 g, 1.21 mmol) was added to the solution. The reaction was allowed to run at room temperature for 24 h and then the insoluble dicyclohexylurea was removed by filtration. The product was then precipitated with diethyl ether, filtered, and vacuum-dried at room temperature to obtain Boc-ss-PEG-ss-Boc with a yield of 2.1 g and the following ^{1}H NMR δ (ppm) spectral characteristics: 4.24 (t, 2H, –OCH_2CH_2O(CO)–), 3.66 (PEG), 2.82 (d, 2H, –(CO)NH$CH_2CH_2SSCH_2CH_2$–), 2.76 (d, 2H, –(CO)NHCH$_2$CH$_2$SSCH$_2CH_2$–), 2.68 (s, 2H, –(CO)NHCH$_2CH_2$SSCH_2CH$_2$–), 2.65 (s, 2H, –(CO)CH$_2CH_2$(CO)NH–), 2.50 (t, 2H, –(CO)CH_2CH$_2$(CO)NH–), 1.43 (s, 9H, –O(CH_3)$_3$).

α,ω-Cystamine- modified PEG (NH_2-ss-PEG-ss-NH_2): Boc-ss-PEG-ss-Boc (2 g, 0.5 mmol) was dissolved in anhydrous dichloromethane (20 mL) and TFA (10 mL). The reaction was allowed to proceed at room temperature for 3 h, the reaction solvent was evaporated, and then the resulting product was precipitated in an excess amount of cold diethyl ether. The precipitate was filtered, washed several times with diethyl ether, and vacuum-dried to obtain NH_2-ss-PEG-ss-NH_2 with a yield of 1.77 g. The ^{1}H NMR δ (ppm) spectral characteristics were 4.24 (t, 2H, –OCH_2CH_2O(CO)–), 3.66 (PEG), 2.96 (t, 2H, –(CO)NHCH$_2$CH$_2$SSCH$_2CH_2NH_2$), 2.77 (t, 2H, –(CO)NHCH_2CH$_2$SSCH$_2$CH$_2$NH$_2$), 2.75 (d, 4H, –(CO)NHCH$_2CH_2$SSCH_2CH$_2$NH$_2$), 2.62 (s, 2H, –(CO)CH$_2CH_2$(CO)NH-), 2.60 (t, 2H, –(CO)CH_2CH$_2$(CO)NH–).

α,ω-Cholesteryl-modified PEG (Chol-ss-PEG-ss-Chol): a mixture of NH_2-ss-PEG-ss-NH_2 (1.5 g, 0.38 mmol), TEA (0.1 g, 0.99 mmol), and tetrahydrofuran (THF, 20 mL) was cooled to 0 °C, and then cholesteryl chloroformate (0.35 g, 0.78 mmol) was added. The resulting mixture was stirred at

room temperature for 24 h, and then TEA hydrochloride was filtered off and concentrated. Then, the product was precipitated with diethyl ether, filtered, and vacuum-dried at room temperature to obtain Chol-ss-PEG-ss-Chol with a yield of 1.7 g. The ^{1}H NMR δ (ppm) spectral characteristics were 4.24 (t, 2H, –OCH$_2$*CH$_2$*O(CO)–), 3.66 (PEG), 2.84 (d, 4H, –(CO)NH*CH$_2$*CH$_2$SSCH$_2$*CH$_2$*NH–), 2.70 (d, 4H, –(CO)NHCH$_2$*CH$_2$*SS*CH$_2$*CH$_2$NH$_2$), 2.69 (m, 4H, –(CO)*CH$_2$*CH$_2$*(CO)NH–), 1.22 (s, 3H, CH$_3$ of cholesteryl), 1.02 (s, 3H, CH$_3$ of cholesteryl), 0.94 (d, 3H, CH$_3$ of cholesteryl), 0.89 (t, 3H, CH$_3$ of cholesteryl), 0.69 (s, 3H, CH$_3$ of cholesteryl).

2.4. Micellization and CMC Measurement of Chol-ss-PEG-ss-Chol

For the micellization of Chol-ss-PEG-ss-Chol, the polymer (10 mg) was dissolved in distilled water (10 mL) and the resulting solution was stirred for 6 h to yield colloidally-stable micellar aggregates in aqueous solution at 1 mg/mL. The CMC of Chol-ss-PEG-ss-Chol micelles was determined using pyrene as a fluorescence probe. The concentration of Chol-ss-PEG-ss-Chol varied from 1×10^{-4} to 1 mg/mL and the pyrene concentration was fixed at 0.6 mM. The prepared samples were incubated with stirring at 37 °C for 36 h to equilibrate the partitioning of pyrene between the water and micelles. The fluorescence spectra were measured using a fluorescence spectrometer (Varian Cary Eclipse) at an emission wavelength of 390 nm. The CMC was estimated from the inflection point of the intensity ratio I_{337}/I_{333} at the various concentrations.

2.5. Reductive Cleavage of Chol-ss-PEG-ss-Chol in Response to DTT

Chol-ss-PEG-ss-Chol micelles (2 mg/mL, 10 mL) were mixed with DTT (15.5 mg, 10 mM) with stirring for 6 h at room temperature. The sample was extracted with diethyl ether to remove the DTT and detached cholestryl moieties, and then the residue remaining in the water was lyophilized, and the reductive cleavage of Chol-ss-PEG-ss-Chol was measured using NMR and GPC analyses. The aqueous Chol-ss-PEG-ss-Chol micellar dispersion (1 mg/mL, 10 mL) was treated with 10 mM DTT with stirring for 6 h and DLS analysis was carried out to determine the size and size distribution.

2.6. Determination of Loading Level of DOX

DOX-loaded micelles were prepared using different feed ratios ($\text{Mass}_{\text{DOX}}/\text{Mass}_{\text{polymer}}$ = 0.1, 0.2, 0.3, and 0.5). Briefly, DOX (0.5 mg) was dissolved in DMF (0.5 mL) with Chol-ss-PEG-ss-Chol (5 mg) and then 5 mL phosphate-buffered saline (PBS, pH 7.4) and TEA (2 mol equivalent to DOX) was added to the solution while stirring at room temperature and the predetermined amounts of DOX were similarly prepared. Then, after stirring for 6 h, the solution was filtered through a syringe filter (0.2 μm pore size) and dialyzed (MWCO: ~2 kDa) against PBS for three days to remove any unloaded DOX and DMF, and the external water source was changed twice a day. The DOX-loaded micelles were freeze-dried and re-dissolved in DMF (4 mL), followed by UV-VIS spectral analysis. A calibration curve ($Y = 19.4889X - 0.00419$, $R^2 = 0.998$) was obtained using varying concentrations of DOX in DMF, and the DOX loading content was calculated by the weight ratio of loaded DOX to dried sample.

2.7. Thiol-Mediated Release of DOX from DOX-Loaded Micelles

DOX release from the DOX-loaded micelles was investigated at 37 °C in PBS with or without DTT. Briefly, 20 mL of aliquots of the DOX-loaded Chol-ss-PEG-ss-Chol micellar dispersion ($\text{Mass}_{\text{DOX}}/\text{Mass}_{\text{polymer}}$ = 0.3,) were introduced into a dialysis tube with cuf-off ~2 kDa, and the dialysis bags were immersed in PBS buffer solution (100 mL) as a control and aqueous DTT solution (10 mM) buffered with PBS. The release medium was shaken at 120 rpm at 37 °C. At predetermined intervals, 3 mL samples were withdrawn from the release medium, and an equivalent volume of fresh medium was subsequently added. The DOX concentration was measured using a UV-VIS spectrometer.

2.8. Cytotoxicity of Micelles

KB cells were grown in EMEM supplemented with 10% FBS, maintained at 37 °C exposed to 5% CO_2 in a humidified incubator, and the medium was changed every other day. To prepare the KB cells for determining the cytotoxicity of the polymers, they were first seeded at a density of 1×10^3 cells/well in 96-well plates in 100 μL of medium and incubated for 24 h. Then, the cells were treated with micelles at different concentrations (0–100 μg/mL) in culture media for 24 h, while cells cultured in medium and PBS were used as the control. The cytotoxicity was finally determined using a CCK-8 kit following the manufacturer's instructions. Briefly, 10 μL of CCK-8 reagent was added to each well of the culture plates with the previously pretreated cells, and then incubated at 37 °C for 2 h. This was followed by detection of the absorbance at 450 nm using a Multiskan microplate reader (Thermo Fisher Scientific Inc., Waltham, MA, USA). The cytotoxicity was expressed as percentage viability of treated cells relative to that of the control cells. All the experiments were performed in *triplicate*, and the data are represented as means ± standard deviation (S.D).

2.9. Intracellular DOX Release

To estimate the effect of GSH on the cytotoxicity of DOX-loaded micelles, the intracellular level of GSH was first manipulated by adding GSH-OEt to the cell culture media. Then, KB cells (100 μL) were evenly seeded into a 96-well plate at a density of 1×10^3 cells/well and incubated for 24 h. The cells were first treated with GSH-OEt (zero, one, and 10 mM) for 3 h, followed by washing with PBS and fresh culture medium. Then, DOX-loaded micelles were added to attain final DOX concentrations of zero, 0.1, 0.2, 0.4, and 0.8 μg/mL for zero, one, and 10 mM GSH-OEt pretreated cells. After incubation for 24 h, the cytotoxicity of the DOX-loaded micelles was evaluated using the CCK-8 assay and free DOX was also similarly determined as a reference for the cytotoxicity.

2.10. Cellular Uptake Determination Using CLSM

To observe the cellular uptake of DOX-loaded micelles, KB cells were seeded in a 35 mm glass-bottom dish (SPL Life Science, Pocheon-Si, Korea) at a density of 5×10^4 cells/mL, cultured for 24 h, and then treated with GSH-OEt (0 and 10 mM) for 3 h. Then, the medium was replaced, and DOX-loaded micelles were added to the cells at a concentration of 0.8 μg/mL. After 3 h, the cells were washed thrice with PBS, stained with 4′,6-diamidino-2-phenylindole (DAPI), and then fixed with 2.5% glutaraldehyde in PBS for 1 h before observation under a confocal laser scanning microscope (CLSM, FV1200, Olympus, Nagano, Japan). The excitation was performed at 405 nm using the same laser light intensity and gain value for all samples while the emission was measured at 461 and 564 nm for DAPI and DOX, respectively.

2.11. Statistical Analysis

The values were expressed as means ± standard deviation (SD). Statistical analysis was performed using the Student's *t*-test with a commercially available program (Sigma plot ver. 12.3, Systat Software, Inc., Chicago, IL, USA).

3. Results and Discussion

3.1. Synthesis and Characterization of Chol-ss-PEG-ss-Chol

The PEG-cholesteryl conjugate containing disulfide linkages was prepared, as illustrated in Scheme 1. PEG was reacted with succinic anhydride to obtain α, ω-carboxylic-modified PEG (HOOC-PEG-COOH). α,ω-(Mono-Boc-cystamine)-modified PEG was prepared by amidation of HOOC-PEG-COOH and mono-Boc-cystamine by a DCC coupling reaction, followed by treatment with TFA to generate α,ω-cystamine-modified PEG. By comparing the integral of the methyl protons in succinyl and cystamine groups, the degree of conjugation of cystamine to HOOC-PEG-COOH was

calculated to be approximately 96.4%. α,ω-Cholesteryl-modified PEG (Chol-ss-PEG-ss-Chol) was obtained through the reaction of cholesteryl chloroformate and α,ω-cystamine-modified PEG. The chemical structure of the resulting PEG-cholesteryl conjugate was characterized using the ^{1}H NMR spectrum. As shown in Figure 1, five strong peaks were evident at 1.22, 1.02, 0.94, 0.89, and 0.69 ppm in the ^{1}H NMR spectrum and assigned to the protons of CH_3 in the cholesteryl group. The peak at 2.69 ppm was attributed to the protons of the succinyl group (–OC(O)CH_2CH_2C(O)–) attached to the PEG chain while the peaks at 2.84 and 2.82 ppm belong to the protons of cystamine (–CH_2CH_2SS–). The cholesteryl groups introduced into α,ω-cystamine-modified PEG was calculated to be approximately 91.7% by comparing the defined peak integral of protons in the succinyl (2.69 ppm) and the protons of CH_3 in the cholesteryl group (0.69 ppm). The number-average molecular weight of Chol-ss-PEG-ss-Chol was 5.58 × 10^3 g/mol with a PDI value of 1.08 determined using GPC with a polystyrene standard. Considering the molecular weight of PEG and cholesteryl units, the theoretically-calculated molecular weight was approximately 4.8 × 10^3 g/mol and the discrepancy between the calculated molecular weight and GPC measured molecular weight may be attributed to the difference in the hydrodynamic property between the Chol-ss-PEG-ss-Chol and the polystyrene standard.

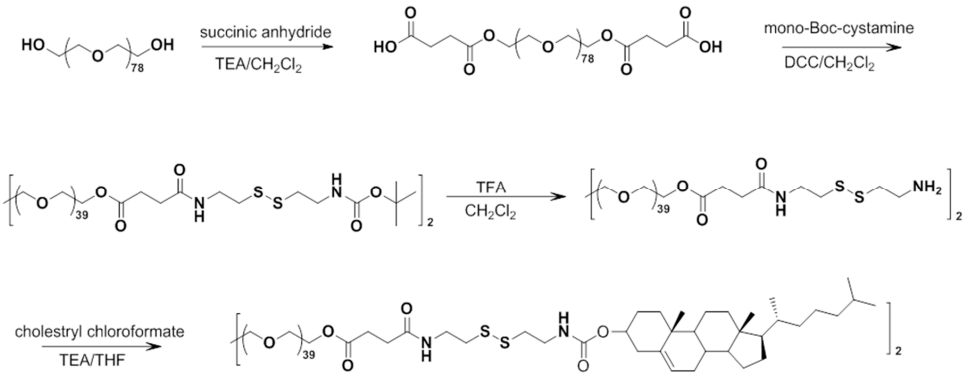

Scheme 1. Synthetic route for poly(ethylene glycol)-cholesteryl conjugate (Chol-ss-PEG-ss-Chol).

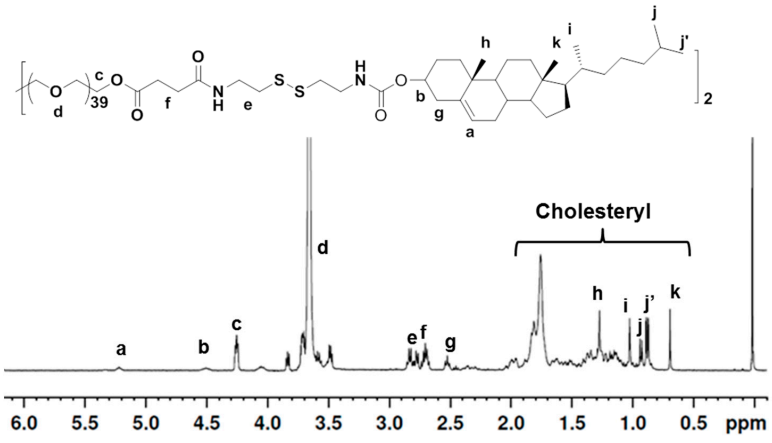

Figure 1. ^{1}H NMR spectrum of poly(ethylene glycol)-cholesteryl conjugate (Chol-ss-PEG-ss-Chol) measured in $CDCl_3$.

3.2. Characterization of Chol-ss-PEG-ss-Chol Micelles

The amphiphilic Chol-ss-PEG-ss-Chol polymers composed of hydrophilic PEG and hydrophobic cholesteryl units were self-assembled into nanometer aggregates in the aqueous solution. The formation of Chol-ss-PEG-ss-Chol micelles was confirmed by fluorescence spectroscopy using pyrene

as a probe. The fluorescence spectra of pyrene with different concentration of Chol-ss-PEG-ss-Chol were shifted from 333 to 337 nm when the concentration of Chol-ss-PEG-ss-Chol increased from 1×10^{-4} to 0.1 mg/mL (Figure 2a). This shift suggests that the pyrene molecules were transferred from the water to the hydrophobic core, indicating the formation of micelles. The plot of the intensity ratio I_{337}/I_{333} against the logarithm of Chol-ss-PEG-ss-Chol concentration is shown in Figure 2b. The intensity ratios remained almost unchanged at a low polymer concentration and began to increase linearly with increasing concentration. The CMC value of Chol-ss-PEG-ss-Chol was calculated graphically from the intersection of the baseline and the increasing line. From the molecular weight as determined by the GPC, the CMC of the prepared polymeric micelles was calculated to be 9.1×10^{-7} M.

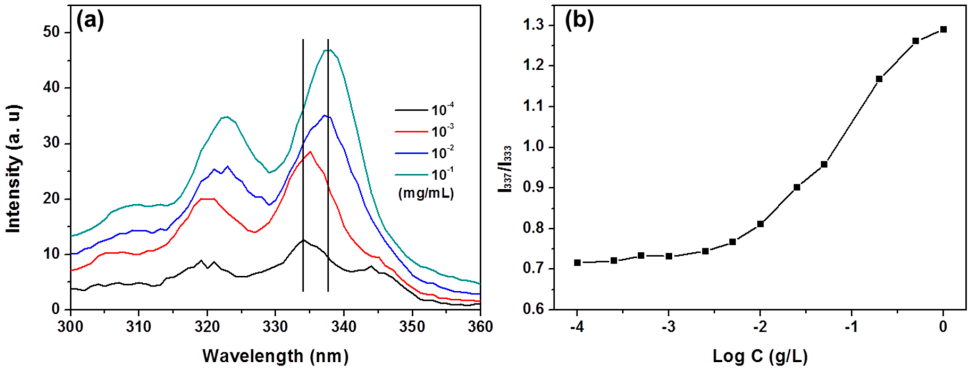

Figure 2. (**a**) Fluorescence excitation spectra of pyrene in aqueous poly(ethylene glycol)-cholesteryl conjugate (Chol-ss-PEG-ss-Chol); and (**b**) intensity ratios (I_{337}/I_{333}) of Chol-ss-PEG-ss-Chol as a function of log concentration.

An adequate micelle size is one of the prerequisites for effective intracellular drug delivery, and micelles with a diameter smaller than 200 nm have shown outstanding advantages, such as reduced reticuloendothelial system (RES) and extended blood circulation half-lives [28,29]. The size of the Chol-ss-PEG-ss-Chol micelles was determined using DLS measurement. As shown in Figure 3, the size distribution of the micelles in aqueous solution exhibited a monomodal distribution with an average diameter of 18.6 nm and a PDI of 0.38. In addition, the size and morphology of Chol-ss-PEG-ss-Chol micelles were determined using TEM and the image shows that the Chol-ss-PEG-ss-Chol self-assembled into approximately spherical micelles in water, and their average diameter was close to the results obtained for the DLS measurement. These results indicate that the size of Chol-ss-PEG-ss-Chol micelles is suitable for intracellular drug delivery.

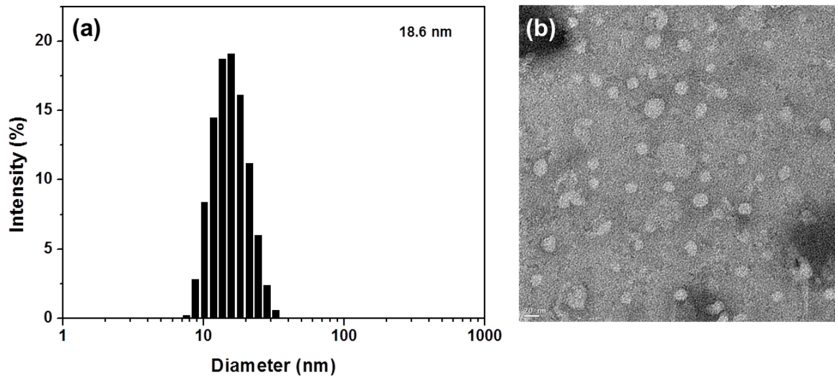

Figure 3. (**a**) Dynamic light scattering (DLS) diagram of poly(ethylene glycol)-cholesteryl conjugate (Chol-ss-PEG-ss-Chol) micelles; and (**b**) transmission electron microscopy (TEM) image negatively stained with phosphotungstic acid hydrate (scale bar, 20 nm).

3.3. Thiol-Responsive Degradation of Chol-ss-PEG-ss-Chol

The disulfide linkage between the hydrophilic PEG and hydrophobic cholesteryl groups confers Chol-ss-PEG-ss-Chol micelles with reductive cleavability in response to reducing agents. To investigate the cleavage of disulfide linkages of the Chol-ss-PEG-ss-Chol micelles in the presence of a reducing agent, they were treated with 10 mM DTT for 6 h, and then DTT and detached cholesteryl moieties were extracted with diethyl ether, and PEG dissolved in water was lyophilized. Each sample was analyzed using ^{1}H NMR and GPC and Figure 4 shows the ^{1}H NMR spectra of Chol-ss-PEG-ss-Chol before and after the exposure to DTT. The proton peak (2.84 ppm, –$CH_2CH_2SSCH_2CH_2$–) adjacent to disulfide disappeared due to the cleavage of the disulfide bond in the presence of DTT. In addition, the proton peaks of DTT and the detached cholesteryl moieties were distinctly observed for the sample extracted with diethyl ether. Although a close observation of spectrum (b) showed the existence of unreacted Chol-ss-PEG-ss-Chol without thiol-disulfide exchange reaction after DTT treatment for 6 h, the cleavage of the disulfide bond in the presence of DTT was confirmed using NMR analysis. Figure 5 shows the GPC curves of the Chol-ss-PEG-ss-Chol before and after treatment with DTT, and values showed a decrease in the molecular weight (M_n) from 5.48 to 4.35 kg/mol (before and after, respectively). Considering the molecular weight of PEG (3.4 kg/mol) and reduced Chol-ss-PEG-ss-Chol (4.35 kg/mol), GPC data showed that Chol-ss-PEG-ss-Chol in the presence of DTT was partially reduced and the peak intensity corresponding to cholesteryl appeared at the retention time of 26 min after treatment with DDT. The ^{1}H NMR and GPC results suggest that the disulfide linkages were cleaved in the presence of DTT.

In addition, DLS and TEM were used to monitor the change in the size distribution of Chol-ss-PEG-ss-Chol micelles in the absence and presence of 10 mM DTT. The average micelle size increased from 18.6 to 355 nm after treatment with DTT, which led to the formation of large aggregates (Figure 6). As shown in the inset of Figure 6, the micelle solution became turbid after treatment with DTT compared with the untreated control solution. This phenomenon can be attributed to aggregation induced by the hydrophobic interaction of non-soluble cholesteryl groups in water after the detachment of the hydrophilic PEG shells from micelles in the presence of DTT. In addition, the TEM image shows that shedding of the PEG shell and aggregation of cholesteryl groups by the cleavage of disulfide linkages resulted in the formation of non-uniform aggregates. These results suggest that the shedding of Chol-ss-PEG-ss-Chol micelles in response to thiols destabilized and disintegrated the micellar aggregates. Furthermore, it is expected that encapsulated drug in micelles can be easily released by destabilization that occurs following shedding of micelles through cleavage of the disulfide linkages mediated by a reducing agent.

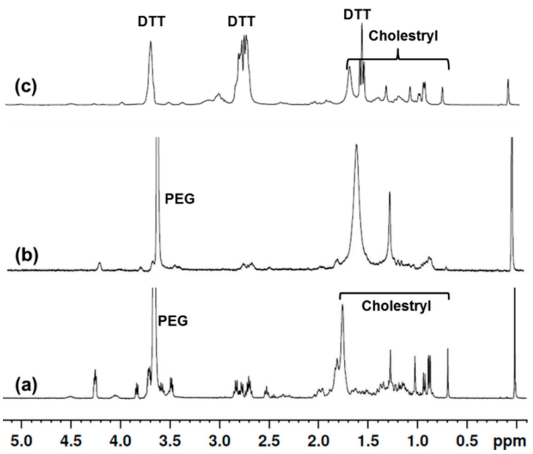

Figure 4. (**a**) ^{1}H NMR spectra of poly(ethylene glycol)-cholesteryl conjugate (Chol-ss-PEG-ss-Chol) measured in $CDCl_3$; and (**b**) lyophilized sample after DL-dithiothreitol (DTT) treatment; (**c**) Mixture extracted with diethyl ether after DTT treatment.

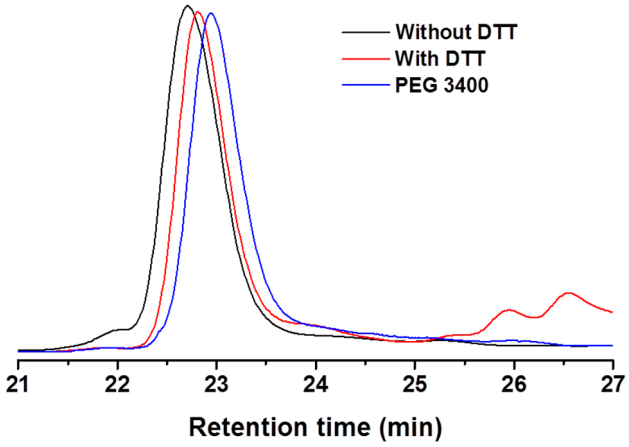

Figure 5. Gel permeation chromatography (GPC) traces of PEG and Chol-ss-PEG-ss-Chol before and 6 h after treatment with 10 mM DL-dithiothreitol (DTT).

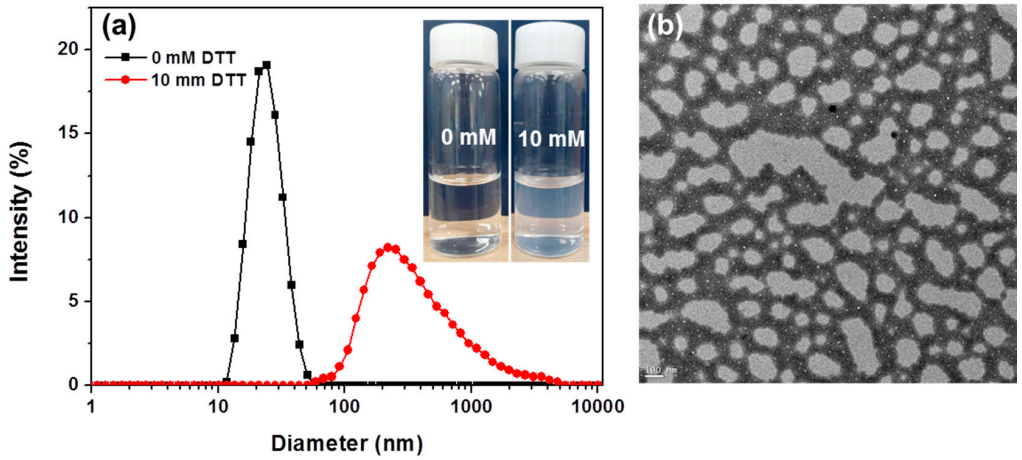

Figure 6. (**a**) Dynamic light scattering (DLS) plots of poly(ethylene glycol)-cholesteryl conjugate (Chol-ss-PEG-ss-Chol) micelles incubated in aqueous buffer solution (control) and 10 mM DL-dithiothreitol (DTT) buffer for 6 h (inset shows digital photographs before and after 10 mM DTT treatment); and (**b**) transmission electron microscopy (TEM) image negatively stained with phosphotungstic acid hydrate after DTT treatment (scale bar, 100 nm).

3.4. Drug Loading and DOX Release upon Thiol-Responsive Destabilization from DOX-Loaded Micelles

DOX, which is a DNA-interacting anticancer drug, was encapsulated in the hydrophobic micellar core of the PEG-cholesteryl conjugate as described in Section 2.6. When the feed ratio of polymer to DOX was 1:0.3, the loaded drug content in Chol-ss-PEG-ss-Chol micelles and corresponding drug loading efficiency were 1.47% and 14.9%, respectively The size and size distribution of the DOX-loaded micelles were determined using DLS and TEM (Figure S1). The size based on the intensity size distribution determined via DLS was in the range of 10–50 nm while the average diameter was 20.4 nm. The TEM image shows that the mean diameter of the DOX-loaded micelles was similar to the results obtained for the DLS measurement. The release of DOX from DOX-loaded micelles following redox-cleavage of the disulfide linkage was also investigated. The *in vitro* drug release from DOX-loaded micelles was determined at 37 °C in PBS containing 10 mM DTT, and DOX release was monitored at predetermined time intervals for 12 h (Figure 7). As a control, the drug release experiment was also performed without DTT, which showed that less than 9% of the encapsulated DOX was released over 6 h, suggesting the drug was released by diffusion from intact micellar aggregates rather than by redox-triggered disassembly of micelles because DOX was

confined in the hydrophobic core of the micelles. However, in the presence of DTT, DOX release from the DOX-loaded micelles was higher than it was in the absence of DTT, owing to the destabilization of Chol-ss-PEG-ss-Chol micelles by the reductive cleavage of disulfide linkages. Approximately 80% of the encapsulated DOX was released from the micelles following DTT treatment. Therefore, the *in vitro* drug release results indicate that the disulfide linkage in Chol-ss-PEG-ss-Chol micelles can be reduced and broken in the reducing environment, which destabilizes the micellar aggregates and accelerates the drug release.

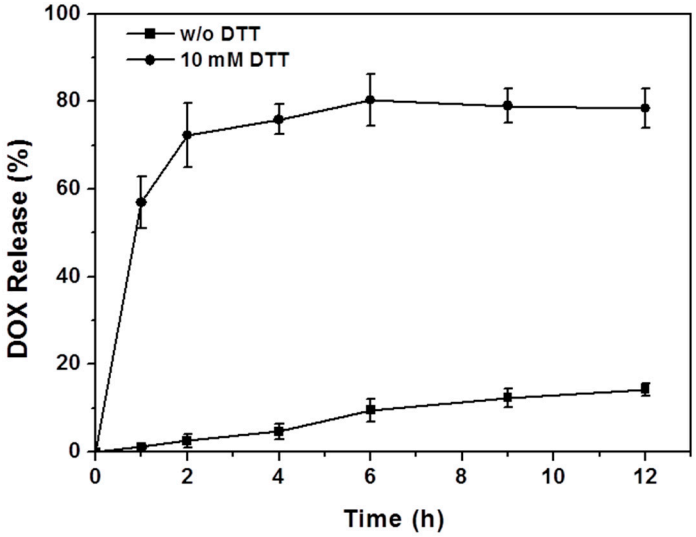

Figure 7. *In vitro* release of doxorubicin (DOX) from DOX-loaded micelles in phosphate buffered saline (PBS) at 37 °C without (w/o) or with 10 mM DL-dithiothreitol (DTT) treatment. Data are mean ± standard deviation (SD), $n = 3$.

3.5. Cytotoxicity of Micelles and Intracellular DOX Release

The CCK-8 assay was used to investigate the cytotoxicity of empty and DOX-loaded micelles. The viability of KB cells was not significantly affected by incubation with varying concentration of Chol-ss-PEG-ss-Chol micelles for 24 h (Figure 8). This result indicates that Chol-ss-PEG-ss-Chol micelles are not cytotoxic to KB cells at concentrations up to 100 μg/mL. In our previous experiment, we reported that treatment with 10 mM GSH-OEt alone for up to 48 h did not affect the viability of KB cells [24]. The cytotoxicity of DOX-loaded Chol-ss-PEG-ss-Chol micelles was evaluated in KB cells with the various cellular GSH forms to investigate whether drug release by the degradation of micelles through the cleavage of disulfide linkages would enhance cytotoxicity. GSH, which has an anionic nature, is not effectively transported across cellular membranes. It has been reported that GSH-OEt, a neutralized form of GSH, penetrates cellular membranes and can be rapidly hydrolyzed in the cytoplasm to generate GSH [30]. KB cells were pretreated with zero, one, and 10 mM GSH-OEt for 3 h and then incubated with various amounts of DOX-loaded micelles for 24 h, while additional cells were incubated with free DOX for comparison. As shown in Figure 8b, the viability of KB cells was decreased concentration-dependently by DOX, indicating it inhibited cell proliferation. In addition, the viability of KB cells pretreated with GSH-OEt was lower than that of the untreated cells. The cell proliferation of DOX-loaded micelles without GSH-OEt pretreatment was reduced to 92% of the control cells at 0.8 μg/mL DOX concentration in micelles; however, pretreatment with 10 mM GSH-OEt decreased the cell proliferation to 80% and 75% of control cells at 0.4 and 0.8 μg/mL DOX concentrations, respectively. Although there is a possibility of free DOX due to degradation of DOX-loaded micelles by the trace amount of GSH-OEt diffused from the inside of cells after the uptake of GSH-OEt, these results indicate that the addition of GSH-OEt increased the intracellular

GSH concentration, which effectively cleaved the disulfide bonds, destabilized the micelles, and facilitated the release of DOX from DOX-loaded micelles into the cytosol.

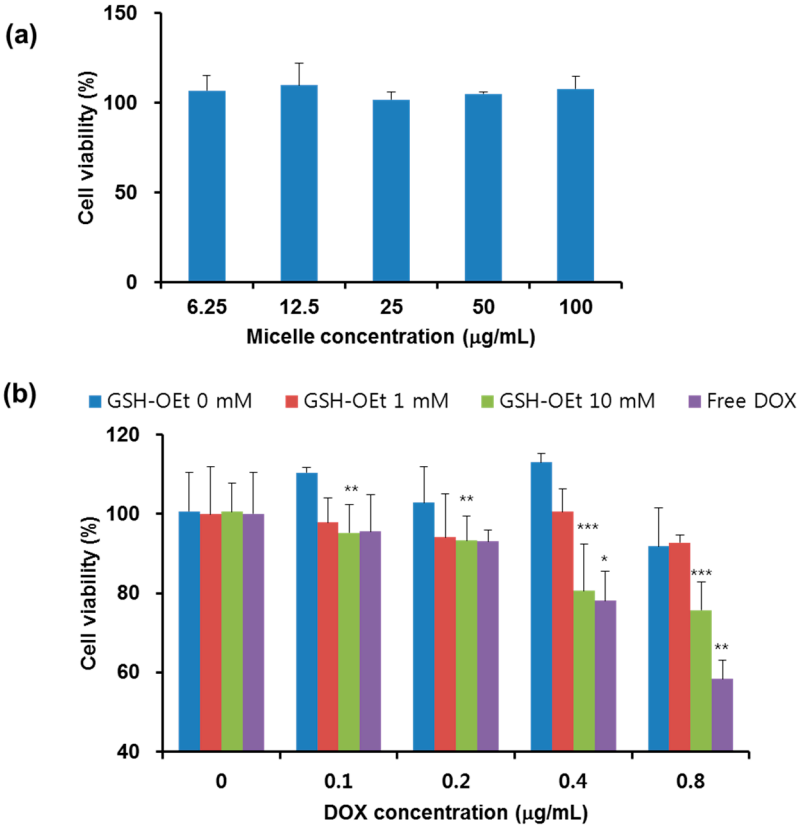

Figure 8. (**a**) KB cell viability after incubation with different concentrations of poly(ethylene glycol)-cholesteryl conjugate (Chol-ss-PEG-ss-Chol) micelles for 24 h; and (**b**) KB cell viability after pretreatment with and without glutathione reduced ethyl ester (GSH-OEt), followed by incubation with different concentrations of free doxorubicin (DOX) and DOX-loaded Chol-ss-PEG-ss-Chol micelles for 24 h. Results are mean ± standard deviation (SD), $n = 3$ (* $p < 0.05$, ** $p < 0.01$, and *** $p < 0.001$).

3.6. Cellular Uptake

The cellular uptake and intracellular release of DOX in response to cellular GSH in KB cells were studied using CLSM. In our experiments, KB cells were pretreated with 0 and 10 mM GSH-OEt for 3 h and then incubated with DOX-loaded micelles and free DOX for 3 h. The localization of DOX within the cells was evaluated using the red auto- and blue fluorescence from DOX and DAPI, respectively. As shown in Figure 9, DOX was distributed in cells and free DOX was observed in the nucleus, showing that it penetrated the nuclear membrane. The DOX in cells incubated with DOX-loaded micelles without pretreatment was distributed in the cytoplasm surrounding the nuclei. However, DOX was more highly distributed in the nucleus of KB cells pretreated with 10 mM GSH-OEt than it was in the untreated cells. The intensity profile of DAPI and DOX (Figure S2) provide evidence that the nuclear distribution of DOX was increased following 10 mM GSH-OEt pre-treatment. These results indicate that the encapsulation of DOX into Chol-ss-PEG-ss-Chol micelles retarded its penetration into the nuclear compartment; however, GSH-mediated degradation of disulfide linkages accelerated intracellular DOX release from the DOX-loaded Chol-ss-PEG-ss-Chol micelles. In addition, the results of the CLSM observation are comparable to those of the cytotoxicity analysis of DOX-loaded micelles in KB cells after pretreatment with one and 10 mM GSH-OEt. The results of the cell viability assay and CLSM suggest that DOX was released from the DOX-loaded micelles

by cleavage of disulfide bonds due to higher intracellular GSH concentrations, which enhanced the inhibition of cell viability.

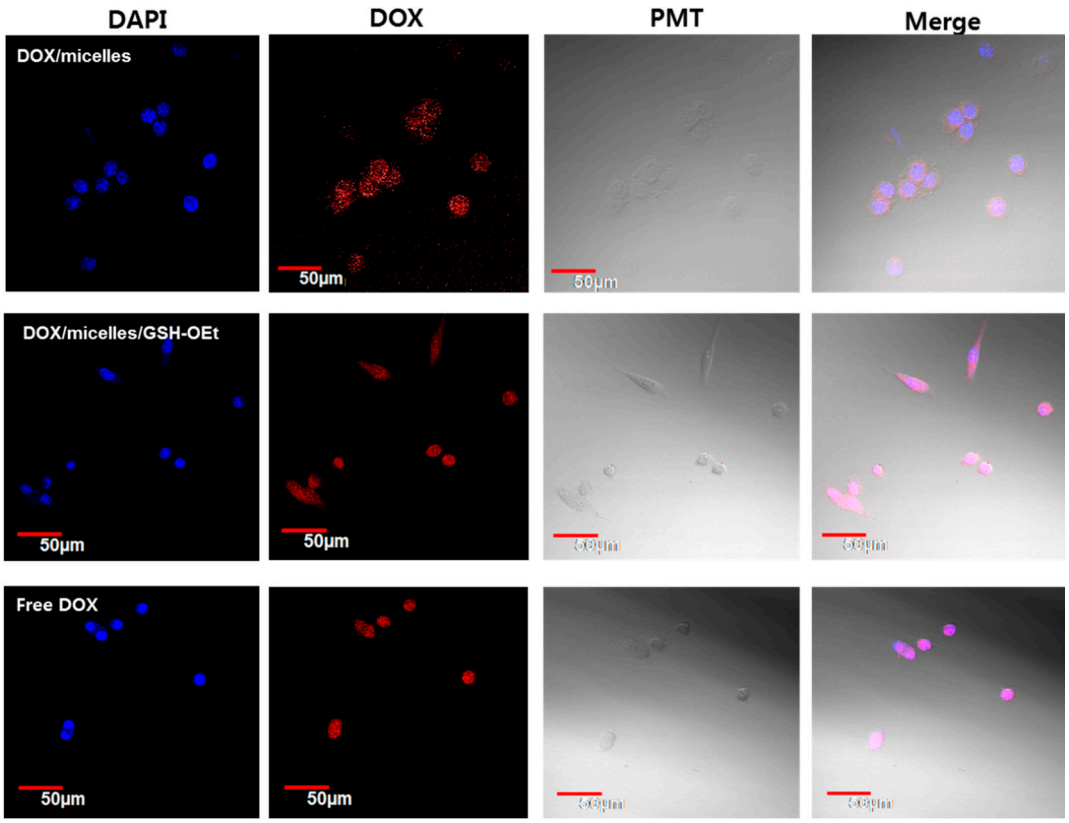

Figure 9. Confocal laser scanning microscopy (CLSM) images of KB cells pretreated with or without glutathione reduced ethyl ester (GSH-OEt) and then incubated with free doxorubicin (DOX) and DOX-loaded Chol-ss-PEG-ss-Chol micelles for 3 h. From left to right: DAPI staining, DOX fluorescence in cells, photomultiplier tube (PMT) images, and overlays of both.

4. Conclusions

We synthesized a stimulus-sensitive micelle, based on Chol-ss-PEG-ss-Chol with disulfide-linkages between the hydrophobic cholesteryl inner core and hydrophobic poly(ethylene glycol) shell, as a thiol-mediated drug delivery carrier. The resulting polymer was characterized using NMR and GPC and the CMC of Chol-ss-PEG-ss-Chol measured using pyrene as a probe was approximately 9.1×10^{-7} M. DLS and TEM measurements confirmed the formation of self-assembled micelles from the Chol-ss-PEG-ss-Chol with an average diameter of 18.6 nm and a PDI of 0.38 due to its amphiphilic structure. Furthermore, NMR and GPC analyses confirmed the cleavage of the disulfide linkage of the Chol-ss-PEG-ss-Chol micelles in the presence the reducing agent, DTT. In addition, the size of DTT-treated micelles was determined using DLS and TEM, which revealed the formation of large aggregates caused by the hydrophobic interaction of the cholesteryl inner core and the detachment of hydrophilic PEG shells through the cleavage of disulfide linkages in the presence of DTT. Moreover, the *in vitro* drug release study showed that DOX was released rapidly following the destabilization of DOX-loaded micelles in the reductive environment. The intracellular release of DOX after internalization into KB cells was confirmed via *in vitro* cell viability assays and CLSM measurements. Therefore, our study demonstrated that the Chol-ss-PEG-ss-Chol micelles were biologically nontoxic and redox-responsive in a reducing environment, suggesting that the amphiphile used in this study has substantial potential for use as an efficient drug delivery system in cancer chemotherapy.

Supplementary Materials: The Supplementary Materials are available online at www.mdpi.com/2073-4360/7/11/1511/s1.

Acknowledgments: This study was supported by the Ministry of Science, ICT, and Future Planning of the Republic of Korea (DGIST Basic Research Fund 15-NB-2).

Author Contributions: Chulsu Baek performed the synthesis, interpreted the experimental results and wrote the paper. Tae-Lin Ha performed the biological experiments and contributed to writing the manuscript. Eunjoo Kim, Sang Won Jeong, Se Guen Lee, and Sung Jun Lee contributed to the discussion section. Hyun-Chul Kim contributed to editing the paper and supervised the entire research project.

Conflicts of Interest: The authors declare no conflict of interest.

References

1. Glen, S.K.; Teruo, O. Polymeric micelles as new drug carriers. *Adv. Drug Del. Rev.* **1996**, *21*, 107–116.
2. Kazunori, K.; Atsushi, H.; Yukio, N. Block copolymer micelles for drug delivery: Design characterization and biological significance. *Adv. Drug Del. Rev.* **2001**, *47*, 113–131.
3. Rodríguez-Hernández, J.; Chécot, F.; Gnanou, Y.; Lecommandoux, S. Toward "smart" nano-objects by self-assembly of block copolymers in solution. *Prog. Polym. Sci.* **2005**, *30*, 691–724. [CrossRef]
4. Vladimir, T.P. Structure and design of polymeric surfactant-based drug delivery systems. *J. Control. Release* **2001**, *73*, 137–172.
5. Moghimi, S.M.; Hunter, A.C.; Murray, J.C. Long-circulating and target-specific nanoparticles: Theory to practice. *Pharmacol. Rev.* **2001**, *53*, 283–318. [PubMed]
6. Bae, Y.H.; Yin, H. Stability issues of polymeric micelles. *J. Control. Release* **2008**, *131*, 2–4. [CrossRef] [PubMed]
7. Ben-Shabat, S.; Kumar, N.; Domb, A.J. PEG-PLA block copolymer as potential drug carrier: Preparation and characterization. *Macromol. Biosci.* **2006**, *6*, 1019–1025. [CrossRef] [PubMed]
8. Xiao, R.Z.; Zeng, Z.W.; Zhou, G.L.; Wang, J.J.; Li, F.Z.; Wang, A.M. Recent advances in PEG–PLA block copolymer nanoparticles. *Int. J. Nanomed.* **2010**, *5*, 1057–1065.
9. Jain, A.K.; Goyal, A.K.; Mishra, N.; Vaidya, B.; Mangal, S.; Vyas, S.P. PEG–PLA–PEG block copolymeric nanoparticles for oral immunization against hepatitis B. *Int. J. Pharm.* **2010**, *387*, 253–262. [CrossRef] [PubMed]
10. Wu, J.; Zhao, J.; Zhang, B.; Qian, Y.; Gao, H.; Yu, Y.; Wei, Y.; Yang, Z.; Jiang, X.; Pang, Z. Polyethylene glycol–polylactic acid nanoparticles modified with cysteine–arginine–glutamic acid–lysine–alanine fibrin-homing peptide for glioblastoma therapy by enhanced retention effect. *Int. J. Nanomed.* **2014**, *9*, 5261–5271.
11. Hwang, M.J.; Suh, J.M.; Bae, Y.H.; Kim, S.W.; Jeong, B. Caprolactonic poloxamer analog: PEG-PCL-PEG. *Biomacromolecules* **2005**, *6*, 885–890. [CrossRef] [PubMed]
12. Diao, Y.-Y.; Li, H.-Y.; Fu, Y.-H.; Han, M.; Hu, Y.-L.; Jiang, H.-L.; Tsutsumi, Y.; Wei, Q.-C.; Chen, D.-W.; Gao, J.-Q. Doxorubicin-loaded PEG-PCL copolymer micelles enhance cytotoxicity and intracellular accumulation of doxorubicin in adriamycin-resistant tumor cells. *Int. J. Nanomed.* **2011**, *6*, 1955–1962.
13. Cuong, N.-V.; Jiang, J.-L.; Li, Y.-L.; Chen, J.-R.; Jwo, S.-C.; Hsieh, M.-F. Doxorubicin-loaded PEG-PCL-PEG micelle using xenograft model of nude mice: Effect of multiple administration of micelle on the suppression of human breast cancer. *Cancers* **2011**, *3*, 61–78. [CrossRef] [PubMed]
14. Machida, Y.; Onishi, H.; Kurita, A.; Hata, H.; Morikaw, A.; Machid, Y. Pharmacokinetics of prolonged-release CPT-11-loaded microspheres in rats. *J. Control. Release* **2000**, *66*, 159–175. [CrossRef]
15. Musumeci, T.; Ventura, C.A.; Giannone, I.; Ruozi, B.; Montenegro, L.; Pignatello, R.; Puglisi, G. PLA/PLGA nanoparticles for sustained release of docetaxel. *Int. J. Pharm.* **2006**, *325*, 172–179. [CrossRef] [PubMed]
16. Ishiwata, H.; Sato, S.B.; Vertut-Doï, A.; Hamashima, Y.; Miyajima, K. Cholesterol derivative of poly(ethylene glycol) inhibits clathrin-independent, but not clathrin-dependent endocytosis. *Biochim. Biophys. Acta* **1997**, *1359*, 123–135. [CrossRef]
17. Dufort, S.; Sancey, L.; Coll, J.-L. Physico-chemical parameters that govern nanoparticles fate also dictate rules for their molecular evolution. *Adv. Drug Deliv. Rev.* **2012**, *64*, 179–189. [CrossRef] [PubMed]

18. He, Z.-Y.; Chu, B.-Y.; Wei, X.-W.; Li, J.; Edwards, C.K.; Song, X.-R.; He, G.; Xie, Y.-M.; Wei, Y.-Q.; Qian, Z.-Y. Recent development of poly(ethylene glycol)-cholesterol conjugates as drug delivery systems. *Int. J. Pharm.* **2014**, *469*, 168–178. [CrossRef] [PubMed]
19. Saito, G.; Swanson, J.A.; Lee, K.-D. Drug delivery strategy utilizing conjugation via reversible disulfide linkages: Role and site of cellular reducing activities. *Adv. Drug Deliv. Rev.* **2003**, *55*, 199–215. [CrossRef]
20. Jonesa, D.P.; Carlson, J.L.; Samiec, P.S.; Paul, S.J.; Vino, C.M.J.; Reed, R.L.; Brown, L.A.S. Glutathione measurement in human plasma evaluation of sample collection, storage and derivatization conditions for analysis of dansyl derivatives by HPLC. *Clin. Chim. Acta* **1998**, *275*, 175–184.
21. Sun, Y.; Yan, X.; Yuan, T.; Liang, J.; Fan, Y.; Gu, Z.; Zhang, X. Disassemblable micelles based on reduction-degradable amphiphilic graft copolymers for intracellular delivery of doxorubicin. *Biomaterials* **2010**, *31*, 7124–7131. [CrossRef] [PubMed]
22. Li, J.; Huo, M.; Wang, J.; Zhou, J.; Mohammad, J.M.; Zhang, Y.; Zhu, Q.; Waddad, A.Y.; Zhang, Q. Redox-sensitive micelles self-assembled from amphiphilic hyaluronic acid-deoxycholic acid conjugates for targeted intracellular delivery of paclitaxel. *Biomaterials* **2012**, *33*, 2310–2320. [CrossRef] [PubMed]
23. Wang, Y.-C.; Wang, F.; Sun, T.-M.; Wang, J. Redox-responsive nanoparticles from the single disulfide bond-bridged block copolymer as drug carriers for overcoming multidrug resistance in cancer cells. *Bioconjugate Chem.* **2011**, *22*, 1939–1945. [CrossRef] [PubMed]
24. Kim, H.-C.; Kim, E.; Ha, T.-L.; Jeong, S.W.; Lee, S.G.; Lee, S.J.; Lee, B. Thiol-responsive gemini poly(ethylene glycol)-poly(lactide) with a cystine disulfide spacer as an intracellular drug delivery nanocarrier. *Colloid Surf. B Biointerfaces* **2015**, *127*, 206–212. [CrossRef] [PubMed]
25. Boomer, A.J.; Qualls, M.M.; Inerowicz, H.D.; Haynes, R.H.; Patri, V.S.; Kim, J.-M.; Thompson, D.H. Cytoplasmic delivery of liposomal contents mediated by an acid-labile cholesterol-vinyl ether-PEG conjugate. *Bioconjugate Chem.* **2009**, *20*, 47–59. [CrossRef] [PubMed]
26. Chen, D.; Jiang, X.; Huang, Y.; Zhang, C.; Ping, Q. pH-Sensitive mPEG-Hz-cholesterol conjugates as a liposome delivery system. *J. Bioact. Compat. Polym.* **2010**, *25*, 527–542. [CrossRef]
27. Shirazi, R.S.; Ewert, K.K.; Leal, C.; Majzoub, R.N.; Bouxsein, N.F.; Safinya, C.R. Synthesis and characterization of degradable multivalent cationic lipids with disulfide-bond spacers for gene delivery. *Biochim. Biophys. Acta* **2011**, *1808*, 2156–2166. [CrossRef] [PubMed]
28. Allen, T.M.; Cullis, P.R. Drug delivery systems: Entering the mainstream. *Science* **2004**, *303*, 1818–1822. [CrossRef] [PubMed]
29. Allen, C.; Maysinger, D.; Eisenberg, A. Nano-engineering block copolymer aggregates for drug delivery. *Colloid Surf. B Biointerfaces* **1999**, *16*, 3–27. [CrossRef]
30. Mary, E.A.; Alton, M. Glutathione monoesters. *Anal. Biochem.* **1989**, *183*, 16–20.